Size influences the cytotoxicity of poly (lactic-co-glycolic acid) (PLGA) and titanium dioxide (TiO2) nanoparticles

Xiong, Sijing; George, Saji; Yu, Haiyang; Damoiseaux, Robert; France, Bryan; Ng, Kee Woei; Loo, Say Chye Joachim

2012

Xiong, S., George, S., Yu, H., Damoiseaux, R., France, B., Ng, K. W., & Loo, S. C. J. (2013). Size influences the cytotoxicity of poly (lactic-co-glycolic acid) (PLGA) and titanium dioxide (TiO2) nanoparticles. Archives of Toxicology, 87(6), 1075-1086.

https://hdl.handle.net/10356/98977

https://doi.org/10.1007/s00204-012-0938-8

Size influences the cytotoxicity of poly (lactic-co-glycolic acid) (PLGA) and titanium dioxide (TiO_2) nanoparticles

Sijing Xiong[1], Saji George[2, 3], Haiyang Yu[1], Robert Damoiseaux[2], Bryan France[2], Kee Woei Ng[1] and Joachim Say-Chye Loo[1*]

1. School of Materials Science & Engineering, Nanyang Technological University, Block N4.1, 50 Nanyang Avenue, Singapore.
2. California NanoSystems Institute, University of California, Los Angeles, California, United States.

[*]Corresponding authors: Dr. Joachim Say-Chye Loo, Tel: +65-6790-4603, Fax: +65-6790-9081, Email: JoachimLoo@ntu.edu.sg.

3. Centre for Sustainable Nanotechnology, School of Chemical and Life Sciences, Nanyang Polytechnic, Singapore 569824.

Abstract:

The aim of this study is to uncover the size influence of poly (lactic-co-glycolic acid) (PLGA) and titanium dioxide (TiO_2) nanoparticles on their potential cytotoxicity. PLGA and TiO_2 nanoparticles of three different sizes were thoroughly characterized before *in vitro* cytotoxic tests which included viability, generation of reactive oxygen species (ROS), mitochondrial depolarization, integrity of plasma membrane, intracellular calcium influx and cytokine release. Size-dependent cytotoxic effect was observed in both RAW264.7 cells and BEAS-2B cells after cells were incubated with PLGA or TiO_2 nanoparticles for 24 h. Although PLGA nanoparticles did not trigger significantly lethal toxicity up to a concentration of 300 μg/ml, the TNF-α release after the stimulation of PLGA nanoparticles should not be ignored especially in clinical applications. Relatively more toxic TiO_2 nanoparticles triggered cell death, ROS generation, mitochondrial depolarization, plasma membrane damage, intracellular calcium concentration increase, and size-dependent TNF-α release, especially at a concentration higher than 100 μg/ml. These cytotoxic effects could be due to the size-dependent interaction between nanoparticles and biomolecules, as smaller particles tend to adsorb more biomolecules. In summary, we demonstrated that the ability of protein adsorption could be an important paradigm to predict the *in vitro* cytotoxicity of nanoparticles, especially for low toxic nanomaterials such as PLGA and TiO_2 nanoparticles.

Key words: PLGA, TiO_2, nanoparticles, cytotoxicity, nanotoxicity, protein adsorption

1. Introduction

The safety of nanomaterials are receiving more and more attention in this decade (Oberdörster et al. 2005b; Nel et al. 2006), because products based on nanotechnology have penetrated into our daily lives, ranging from cosmetics to medical products (McCall 2011; Nel et al. 2006). However, more attention is paid to soluble metal oxide particles, such as ZnO, that release toxic metal ions like Zn^{2+} (George et al. 2009; Ng et al. 2011; Heng et al. 2010a; Heng et al. 2010b). The potential mechanism of cytotoxicity induced by non-soluble metal oxide such as TiO_2 nanoparticles and biomedical nanomaterials is still controversial. TiO_2 nanoparticles are even considered as a "natural" nanomaterial and are positively accepted by the general public (Skocaj et al. 2011). However, some reports have pointed out the potential toxicity of TiO_2 nanoparticles, including their ability to induce oxidative stress (Gurr et al. 2005; Kang et al. 2008; Long et al. 2006; Park et al. 2008), genotoxicity (Petkovic et al. 2010; Rahman et al. 2002; Wang et al. 2007), and immunotoxicity (Sayes et al. 2006; Palomaki et al. 2009). However, the mechanism behind these cytotoxic effects is still unclear. Besides these non-soluble metal oxide particles, more attention should also be given to biomedical nanomaterials. Zhao *et al.* (Zhao et al. 2010) reported that hydroxyapatite (HA) nanoparticles of three different surface areas did not cause significant decrease in cell viability, but higher ROS generation was observed in the cells after incubating with HA nanoparticles of large surface areas. PLGA nanoparticles are also widely studied for biomedical applications and have great potential to be used in drug delivery systems. The encapsulation of drugs into PLGA nanoparticles can prevent premature drug degradation, reduce side effects, enhance drug efficacy and achieve desired drug release rates, *etc.* (Dong and Feng 2007; Cartiera et al. 2009). Although more than 1,000 articles, on PLGA nanoparticle as drug delivery systems have been published and indexed in the Web of Science, the number of papers with that reports on its cytotoxicity are fewer than 10. Thus, it is crucial to understand the potential toxicity and cytotoxic mechanism of these nanomaterials. Since the toxicity of nanoparticles is related to their physicochemical properties such as size, shape, chemical composition, surface area, surface chemistry and surface charge *etc.* (Oberdörster et al. 2005a), understanding how these properties can influence cytotoxicity will provide us with useful insights on the possible mechanisms behind their toxicity.

The objective of this study is therefore to investigate the potential cytotoxicity of PLGA and TiO_2 nanoparticles, and how particle size can influence this outcome. Three different-sized PLGA and TiO_2 nanoparticles were investigated. RAW264.7 (murine macrophage) cells were chosen to represent the phagocytic cell lines, which can actively interact with foreign particles in *in vivo* systems (Xia *et al.* 2008; Zhao *et al.* 2010). BEAS-2B (human bronchial epithelial) cells were chosen to represent airway epithelium which is one of the defensive cells against inhaled nanoparticles (Zhao *et al.* 2010). RAW264.7 and BEAS-2B cells are well understood cell line models for nanotoxicology studies (Xia *et al.* 2008; George *et al.* 2009; Zhao *et al.* 2012). We chose these two cell lines to evaluate and understand the cytotoxicity of different-sized PLGA and TiO_2 nanoparticles in order to compare our results with earlier studies. Moreover, in our previous studies, we have successfully used these two cell lines to investigate the cytotoxicity of different surface area of hydroxyapatite (HA) nanoparticles with potential biomedical applications (Zhao *et al.* 2010). Nanoparticles were characterized for their physicochemical properties before *in vitro* cytotoxicity studies. Cytotoxicity parameters tested included cell viability, generation of ROS, mitochondrial depolarization, plasma membrane leakage, increased intracellular calcium concentration and inflammation response. A potential paradigm to explain and predict the cytotoxicity of different sized nanoparticles is proposed in this study.

2. Materials and Methods

2.1 Materials

PLGA (RG502H) was purchased from Boehringer Ingelheim, Germany. PVA of molecular weight 30,000-70,000, acetone, dichloromethane (DCM) were purchased from Sigma-Aldrich, Singapore. The TiO_2 nanoparticles of different sizes were purchased from commercial sources. 10 nm (T10), 20 nm (T20) and 100 nm (T100) TiO_2 nanoparticles were purchased from SkySpring Nanomaterials Inc., Evonik Industries and MKnano Inc., respectively. PYROGENT® Plus single-test with CSE 0.06 EU/ml sensitivity (N289-06) was purchased from Lonza, Singapore. Bronchial Epithelial Cell Growth Medium (BEGM) (cc-3171 and cc-4175) was purchased from Lonza, USA. RAW264.7 (# TIB-71) cells and BEAS-2B (# CRL-9609) cells were purchased from ATCC, USA. Sodium pyruvate and penicilin-streptomycin were purchased from Hyclone, USA. Fetal Bovine Serum (FBS) was from Benchmark, USA. Dulbecco's Modified Eagle Medium (DMEM), Hoechst (H3570), MitoSOX (M36008), JC-1 (T3168),

Propidium Iodide (PI) Nucleic Acid Stain (P3566) and Fluo-4 (F14202) were purchased from Invitrogen, USA. Mouse TNF-α ELISA (#430902) was purchased from Biolegend, Singapore. Pierce 660 nm Protein Assay (#22660) was purchased from Thermo Fisher Scientific, Singapore.

2.2 Synthesis of PLGA nanoparticles

The PLGA nanoparticles were synthesized in-house. The smallest PLGA nanoparticles (60 nm, P60) were synthesized through modified nano-precipitation method (Chorny et al. 2002). In brief, 25 mg PLGA was dissolved in 6 ml of organic solvent mixture (acetone / DCM, 39:1, v/v). The PLGA solution was drop-wisely added into 18 ml 0.125% PVA solution under magnetic stirring at 990 rpm. The organic solvent was removed through magnetically stirring for 24 h. The final colloid was freeze-dried for 48 h.

The 100 nm and 200 nm PLGA nanoparticles (P100 and P200) were synthesized through modified oil in water (o/w) single emulsion solvent evaporation process (Song et al. 2008) using different organic solvent. In brief, 50 mg PLGA was dissolved in 1.5 ml organic solvent or solvent mixture. For P100, the organic solvent mixture composed of DCM and acetone (2/1, v/v). For P200, the organic solvent was chloroform only. 4.5 ml of PVA (1%, w/v) solution was slowly added into the PLGA solution. Microtip probe ultrasonicator (Sonics & materials Inc., USA) was used to ultrasonicate the solution at the oil/water interface with ice water bath for 3 min. The organic solvent was removed through magnetically stirring for 24 h. The final colloid was freeze-dried for 48 h.

2.3 Characterization of nanoparticles

2.3.1 Size and zeta potential measurement

The primary particle sizes of the PLGA and TiO_2 nanoparticles were characterized by using field emission scanning electron microscope (FESEM, Jeol JSM 6340F) and transmission electron microscope (TEM, JOEL 2010), respectively. The dispersed PLGA colloid in water was dropped onto a silica chip and air dried. The silica chip with PLGA nanoparticles was coated with platinum at 20 mA for 70 seconds under vacuum. The images were taken by using FESEM at an acceleration voltage of 2 kV. The dispersed TiO_2 nanoparticles in methanol were dropped onto a

carbon coated copper grids. The TiO_2 nanoparticles were observed under TEM at an accelerating voltage of 200 kV. The particle size was measured by using ImageJ software.

The hydrodynamic size and zeta potential of the particles in water, complete Dulbecco's modified eagle medium (CDMEM) and bronchial epithelial growth medium (BEGM) were measured by using dynamic light scattering (DLS) technique. The stock suspension (3 mg/ml) of nanoparticles was prepared by dispersing the particle powder in deionized water, CDMEM or BEGM. Ultrasonication was conducted in water bath ultrasonicator for 10 min. The colloid was diluted into working suspension at a concentration of 30 μg/ml. The working suspension was ultrasonicated for another 10 min before testing with ZetaPALS zeta potential analyzer (Brookhaven instruments, USA).

2.3.2 Brunauer Emmett Teller (BET) surface area and theoretical surface area

The specific surface area of TiO_2 nanoparticles was tested by the Brunauer Emmett Teller (BET) method. The TiO_2 powder was degassed for 4 h at 200 ^{o}C in flowing nitrogen prior to nitrogen absorption using Micromeritics surface area analyzer (ASAP 2000, USA).

The theoretical surface area was calculated through the equation (1) (Jang et al. 2001).

$$S = {}^{6}/_{\rho d} \qquad \text{equation (1)}$$

S represents the theoretical surface area. ρ is the true density of materials. d represents the mean diameter of nanoparticles. The true density of PLGA and TiO_2 was estimated at 1.357 g/cm^3 (Duvvuri et al. 2005) and 3.900 g/cm^3 (Tanaka and Suganuma 2001) respectively.

2.3.3 X-ray powder diffraction (XRD) test

The crystal structure of three different sized TiO_2 nanoparticles were investigated by XRD (Panalytical X'Pert Prodiffractometer, CuKα radiation). The step size was 0.02° and the counting time was 0.5 s / step over a range of 20°-80° 2θ.

2.4 *In vitro* cell culture study

2.4.1 Cell culture

RAW264.7 cells were cultured in CDMEM containg 88% DMEM, 10% FBS, 1% sodium pyruvate and 1% penicilin-streptomycin. BEAS-2B cells were cultured in BEGM. The cells were sub-cultured at 70-80% confluence about every 3 days and incubated in a humidified atmosphere containing 5% CO_2 at 37 ^oC.

2.4.2 Cell metabolic activity study

RAW264.7 and BEAS-2B cells were seeded in 96-well plate and incubated for 24 h before nanoparticles of different concentrations were added. The cells were incubated with nanoparticles for another 24 h. After the incubation period, the supernatant medium was collected for TNF-α measurement using ELISA (see below). The cells were added with MTS working solution in complete cell culture medium and incubated for 1 h. The whole 96 well plate was centrifuged at 250 g for 10 min in order to spin down nanoparticles that could interfere with the absorbance reading. The supernatant was collected to measure the absorbance at 490 nm using SpectraMax M5e (Molecular Devices Corporation, USA). The absorbance at 690 nm was used as reference.

2.4.3 Multiparametric assay

Cytotoxicity parameters including ROS generation, mitochondrial depolarization, plasma membrane leakage and increased intracellular calcium concentration were tested using high throughput screening platform (George et al. 2009). Three sets of fluorescence probe cocktails were prepared by mixing wavelength-compatible fluorescent probes in PBS. The first cocktail contained 1 μM Hoechst (blue) and 5 μM MitoSOX (red). The second cocktail contained 1 μM Hoechst (blue) and 1 μM JC-1 (red/green). The third cocktail contained 1 μM Hoechst (blue), 5 μM propidium iodide (PI) (red) nucleic acid stain and 5μM Fluo-4 (green). The use of different probes to track cellular responses is summarized in table 1. Cells were seeded in 384-well plate with transparent bottom and incubated for 24 h to allow attachment. Nanoparticles of different concentrations were added and incubated with cells for another 24 h. On the third day, cells were washed twice with PBS, and then incubated with 25μl dye cocktail in the dark for 30 min in 37 ^oC with humidified atmosphere containing 5% CO_2. The fluorescent images were taken automatically using an automated epifluorescence microscope, Image-Xpress^{micro} (Molecular

Devices, Sunnyvale, USA) under 10 × magnifications. The images were automatically analyzed by using Meta-Xpress software to calculate the percentage of cells showing positive signals.

2.4.4 ELISA test for TNF-α and endotoxin test

The TNF-α released into the medium was measured by Mouse TNF-α ELISA following the protocol provided by Biolegend. To exclude the possibility that the inflammation response of cells was due to the stimulation by endotoxin attached on materials, the endotoxin level in nanoparticle samples was tested using PYROGENT® Plus single-test with CSE 0.06 EU/ml sensitivity following the protocol provided by Lonza. The endotoxin test was conducted for all nanoparticles at a concentration of 300 μg/ml.

2.4.5 Nanoparticle-protein adsorption study

Nanoparticles (1 mg/ml) were dispersed in 2 mg/ml bovine serum albumin (BSA) in DMEM solution and ultrasonicated for 20 min. All the particles were collected by centrifugation at 14,000 rpm for 20 min at 25 ^{o}C, and washed thrice with Milli-Q water. The protein attached on PLGA nanoparticles was quantified using Pierce 660 nm Protein Assay following the manufacture's protocol using Bovine Serum Albumin (BSA) as a model protein. The adsorption of protein on TiO_2 nanoparticles was tested using Thermo Gravimetric Analyzer (TGA, 2950, HR, V5.4A). The collected TiO_2 nanoparticles were freeze-dried for 48 h before the TGA test. The curves of weight loss for BSA and BSA adsorbed TiO_2 nanoparticles were obtained at a heating rate of 20 ^{o}C/min in a nitrogen-filled atmosphere.

2.5 Statistics

All quantitative data are shown as the means ± standard deviation (SD). Statistical analysis was conducted by using a one-way analysis of variance (ANOVA) and Tukey's pairwise comparisons. The difference was considered to be significant when $p < 0.05$. * represented the data with significant difference when compared with the control group. # represented the data with significant difference when compared with other particles at the same concentration. All tests were repeated four times.

3. Results and Discussion

3.1 Physical characterization of PLGA and TiO_2 nanoparticles

The characterization data for the particles tested are listed in Table 2. Their SEM and TEM images are shown Figure 1, which reflects the primary size and morphology of PLGA and TiO_2 nanoparticles. The PLGA nanoparticles of three different sizes were spherical with a mean diameter of 61 nm for P60 (a), 94 nm for P100 (b) and 205 nm for P200 (c), which was measured using the SEM images. The TiO_2 nanoparticles of three different sizes were near-spherical particles with primary size 10 nm for T10 (d), 20 nm for T20 (e) and 100 nm (f) for T100 as shown in Figure 1. DLS technique was used to measure the hydrodynamic size and zeta potential of the nanoparticles in both water and complete cell culture medium CDMEM and BEGM (Table 2). The hydrodynamic size was bigger than their primary size. Although different particles showed different surface charge in water, the zeta potentials in CDMEM and BEGM were similar within the range of -2 mV to -13 mV. This could be due to the adsorption of the proteins and ions in the cell culture medium onto the particle surface, resulting in the neutralization of surface charge (Xia *et al.* 2006). The BET method was utilized to quantify the specific surface area of TiO_2 nanoparticles. However, this method was not applicable for PLGA nanoparticles due to the low melting point of PLGA polymer. From the results shown in Table 2, the smallest TiO_2 nanoparticles (T10) had the highest BET surface area (166.0 m^2/g). The experimental BET surface area was close to the theoretical surface areas calculated through the size and true density of the materials (equation 1). These results indicated that smaller particles had larger surface areas. The crystal structure of TiO_2 nanoparticles were tested through XRD. Results show that TiO_2 nanoparticles of three different sizes were mainly anatase. The endotoxin test was conducted to exclude the possibility that the inflammation response of the cells was due to the endotoxin attached on the materials. From table 2, the endotoxin in the materials was lower than 0.06 EU/ml at the highest particle concentration of 300 μg/ml. This result suggested that the inflammation response of the cells could be more likely due to the particles themselves instead of the endotoxin in the samples.

3.2 Limited effect of PLGA and TiO_2 nanoparticles on cell viability

To test the cytotoxicity of PLGA and TiO_2 nanoparticles, the particles of concentrations ranging from 10 μg/ml to 300 μg/ml were incubated with RAW264.7 and BEAS-2B cells for 24 h. For *in vitro* cell viability test, MTS assay was utilized to quantify the metabolically active cells through

the interaction between MTS and dehydrogenase enzymes in live cells. Figure 2 exhibited the metabolic activity of cells after interaction with PLGA (a and b) and TiO_2 (c and d) nanoparticles. The graph indirectly indicates the viability of live cells in each group as compared to the negative control (0 μg/ml). Figure 2a and 2b showed no apparent cytotoxicity for PLGA nanoparticles regardless of the size. This result is consistent with other reports that PLGA nanoparticles do not show obvious acute lethal toxicity to cells within 24 h of incubation (de Lima et al. 2010; Semete et al. 2010). As for TiO_2 nanoparticles, cell viability was generally uncompromised (> 80%) after 24 h exposure (Figure 2c and 2d). However, viability of BEAS-2B cells was statistically lower after they were exposed to 300 mg/ml of T10 and T20 nanoparticles as compared to the negative control (Figure 2d).

3.3 Cells displayed different responses to different sized nanoparticles in the multiparametric assay

There are many biological and molecular reactions happening in cells upon stimulation with nanoparticles (Oberdörster et al. 2005b; Nel et al. 2006). Among them, the oxidative stress stimulated by nanoparticles is considered a useful paradigm to predict the toxicity of nanomaterials (Xia *et al.* 2006). Oxidative stress could trigger a range of oxidant injuries including mitochondrial depolarization, intracellular calcium ion influx and even cause the death of cells (Figure 7) (George et al. 2009). George *et al.* (George et al. 2009) showed that the cytotoxicity events involved in oxidative stress pathway could be measured using fluorescence probes. These dyes were Hoechst, PI, MitoSOX, JC1 and Fluo-4 (George et al. 2009; George et al. 2011; Zhang et al. 2011). Hoechst and PI are two DNA interactive agents. The cell-permeable Hoechst is utilized to bind to DNA of both live and dead cells, allowing us to quantify and locate the total cells in each image. The PI can only penetrate into dead cells through the damaged plasma membrane to indicate the number of dead cells (George et al. 2009). The generation of superoxide in mitochondria can be detected with MitoSOX Red staining. If ROS generation cause oxidative stress in cells, a decrease in mitochondrial membrane potential would be detected using cationic dye JC1, which indicates unhealthy mitochondria (George et al. 2009). JC1 is normally accumulated in the mitochondria of healthy cells. But during mitochondrial depolarization, the dye is released from the mitochondria to the cytosol. This release will cause the fluorescence color to shift from red to green, which forms the basis of quantifying cells with

decreased mitochondrial potential. Fluo-4 is a dye to detect intracellular calcium levels, which fluoresces green when there is an increase in the intracellular calcium ions.

This multiparametric assay was conducted after RAW264.7 and BEAS-2B cells were exposed to different sized nanoparticles for 24 h. The results shown in Figure 3 and Figure 4 indicated the percentage of positive cells for each parameter whose fluorescence intensity was above a certain threshold using Meta-Xpress software. The potential cytotoxic effect of PLGA nanoparticles were shown in Figure 3. Limited damaging response was observed in both of RAW264.7 and BEAS-2B cells after incubation with PLGA nanoparticles (positive cells < 10%). However, the smallest PLGA nanoparticles (P60) triggered similar increase in the intracellular calcium flux in both RAW264.7 and BEAS-2B cells. Calcium is an important regulator of mitochondrial function. The disturbance of cytosolic calcium homeostasis may trigger profound influence on cell functions (Brookes et al. 2004). High concentration of Ca^{2+}, especially in pathology, has negative effect on the function of mitochondria through ROS generation (Brookes et al. 2004). But based on our current results, the slight increase in the calcium concentration in P60 treated cells did not cause obvious cell death or damage of organelles. The TiO_2 nanoparticles exhibited more obvious size and concentration dependent cytotoxicity to both RAW264.7 and BEAS-2B cells (Figure 4). The PI uptake results confirmed the results in MTS tests that only T10 and T20 triggered ~10% cell death at the highest concentration of 300 μg/ml. Size-dependent generation of mitochondrial superoxide was observed in both RAW264.7 and BEAS-2B cells. ROS generation after the interaction with TiO_2 nanoparticles in the *in vitro* studies was also observed in BEAS-2B cells by other groups (Wang et al. 2007; Gurr et al. 2005). Only T10 triggered statistically increased signal in intracellular calcium flux parameter in both RAW264.7 and BEAS-2B cells at the concentration higher than 100 μg/ml. In summary, the results of the multiparametric assay showed that the cytotoxicity of PLGA and TiO_2 nanoparticles was size-dependent and smaller particles tend to trigger higher level of damage to both RAW264.7 and BEAS-2B cells in this *in vitro* investigation.

3.4 PLGA and TiO_2 nanoparticles triggered size and concentration dependent inflammation response.

Nanoparticles have different ways of entering the human body and activating the immune system. PLGA nanoparticles, proposed to be used in biomedical field, were designed to deliver drugs through intravenous administration. As for TiO_2 nanoparticles, although they are more commonly used in sunscreens, they still have great potential to enter human body through lung and gastrointestinal tract (Skocaj et al. 2011). The immune systems in living organisms have many ways to protect themselves from the attacks by "foreign invaders", which include infectious bacteria, virus as well as natural and synthetic materials (Sim and Wallis 2011). The expression of pro-inflammatory cytokines such as TNF-α released from macrophages can be used to indicate the inflammatory responses. TNF-α plays an active role in mediating inflammation, generalized wasting and septic shock (Ziolli and Jardim 2002), programmed cell death (Ziolli and Jardim 2002), and metabolic disturbances in cancer patients (Zhang et al. 2007). TNF-α induction of cytokine cascades can induce and maintain inflammation. Although the evolutionary advantages of inflammatory response could be the resistance to infection, the unnecessary and prolonged inflammation may cause damages to human health. RAW264.7 cells, a kind of macrophage cells, can release cytokines such as TNF-α with the stimulation of materials in the earlier phase of inflammation (Ding 2009). In this study, we tested the TNF-α released from RAW264.7 cells after 24 h incubation with PLGA and TiO_2 nanoparticles (Figure 5). The graph showed an obvious trend that smaller particles tend to trigger more release of cytokine TNF-α from RAW264.7 cells. P60 and P100 nanoparticles started to show statistical difference when compared to control from 10 μg/ml and 100 μg/ml, respectively. The P200 nanoparticles did not trigger significant release of TNF-α up to 300 μg/ml. This result indicated that PLGA nanoparticles with size larger than 100 nm would be safer for biomedical applications. As for TiO_2 nanoparticles, T10 triggered the highest level of cytokine release starting from 10 μg/ml. Both T20 and T100 triggered similar amount of TNF-α release, which showed statistical difference from the control at 100 μg/ml. The TNF-α release stimulated by TiO_2 nanoparticles was also observed by other studies (Palomaki et al. 2009; Tao and Kobzik 2002). TiO_2 could not only trigger the expression of TNF-α but also stimulate the release of other cytokines including IL-6 and MIP-1α in macrophages (Palomaki et al. 2009). The increase in maturation of macrophage and antigen presentation triggered by TiO_2 nanoparticles was also observed in Palomaki *et al.*'s study (Palomaki et al. 2009). Similar trend was also observed by Oberdorster *et al.* from their *in vivo* study (Oberdorster et al. 1992) whereby after intratrachial instillation of

different sized TiO_2 nanoparticles, obvious acute inflammatory response was indicated by the lung lavage parameters. This pulmonary inflammatory response correlated well with surface area of particles instead of particle mass, volume, or numbers, so similarly smaller particles with higher surface area could also trigger higher level of inflammatory response.

3.5 The protein adsorption on PLGA and TiO_2 nanoparticles was size-dependent

All the cytotoxicity studies showed that the cytotoxicity of PLGA and TiO_2 nanoparticles was size-dependent. Unlike other nanomaterials such as ZnO, PLGA and TiO_2 nanoparticles do not release toxic ions like Zn^{2+}. Thus, the potential mechanism behind this cytotoxicity could be due to the size-dependent interaction between nanoparticles and intracellular biomolecules adsorbed onto nanoparticles. Smaller nanoparticles have larger surface area and higher percentage of molecules exposed on particle surface to interact with surrounding biomolecules. To investigate this hypothesis, we studied the adsorption of BSA (a model biomolecule) to different sized PLGA and TiO_2 nanoparticles. Two different methods, Pierce 660 test and TGA analysis were chosen to test the protein adsorption onto PLGA nanoparticles and TiO_2 nanoparticles, respectively. This is because the TiO_2 nanoparticles have strong absorbance at 660 nm which interferes with the absorbance of Pierce 660 reagent. Meanwhile, the PLGA polymer is unstable for TGA analysis. Figure 6a shows the protein quantification of BSA attached on PLGA nanoparticles through Pierce 660 assay. The theoretical surface area of PLGA nanoparticles (per 100 mg) and the amount of BSA adsorbed onto 100 mg PLGA nanoparticles for P60, P100 and P200 were listed in the table of Figure 6 a. The protein adsorption correlated well with the surface area of the PLGA nanoparticles (R^2>0.9). Similar trend was also observed in Figure 6b, which is the TGA result of BSA adsorption onto TiO_2 nanoparticles. The weight decreased more for T10-BSA and T20-BSA when compared with T100-BSA in the temperature range from 188 ^oC to 485 ^oC, which was the major weight loss temperature range of BSA protein. This indicated more BSA adsorbed onto T10 and T20 nanoparticles than on relatively larger T100 nanoparticles. By comparing the results in Figure 6 a and b, 100 mg of P100 nanoparticles could only adsorb 0.441 mg of BSA, but 100 mg of T100 nanoparticles could adsorb more than 2 mg of BSA. This could be the reason for the higher cytotoxicity of 100 nm TiO_2 nanoparticles as compared with 100 nm PLGA nanoparticles. BSA remained attached on these nanoparticles after

extensive washing, which indicated a high-affinity interaction between BSA and nanoparticles especially for TiO_2 nanoparticles.

The data therefore suggests that the size dependent cytotoxicity of PLGA and TiO_2 nanoparticles should be related to different surface area of different-sized nanoparticles. Smaller particles have bigger surface area and more molecules exposed on particle surface to interact with intracellular biomolecules nearby. The potential mechanism of such size-dependent cytotoxicity is shown in Figure 7. When nanoparticles come in to contact with intracellular biomolecules, these biomolecules may adsorb onto the surface of the particles and interact with these "intruder" nanoparticles. These interactions may then trigger a series of responses in cells including generation of reactive oxygen species (ROS), mitochondrial depolarization, plasma membrane leakage, intracellular calcium influx and cytokine release.

Although it has been found that reaction between nanoparticles and proteins is related to some pathological changes such as protein aggregation or unfolding, the mechanism of these damages is still poorly investigated and understood (Deng *et al.* 2011). Some studies have reported that the interaction between nanoparticles and biomolecules could lead to dysfunction or damage of biomolecules (Deng *et al.* 2011; Wang *et al.* 2010; Shang *et al.* 2007; Teichroeb *et al.* 2008). Wang *et al.* (Wang et al. 2010) investigated the interaction between TiO_2 nanoparticles and trypsin. They observed a strong physical adsorption effect of TiO_2 nanoparticles on enzyme trypsin and found inhibitory effect of TiO_2 nanoparticles on trypsin activity by changing the α-helix and β-sheet ratio of the protein structure. Deng *et al.*(Deng *et al.* 2011) found the interaction between poly (acrylic acid) coated gold nanoparticles and fibrinogens would induce the unfolding of protein fibrinogen, which resulted in the activation of Mac-1 reception and inflammation response. Smaller particles (5 nm) tend to bind more fibrinogen than bigger particles (20 nm), and the adsorption is proportional to the surface area of nanoparticles. Wang *et al.* (Wang et al. 2009) reported a sized dependent toxicity of silica nanoparticles on cultured human embryonic kidney (HEK293) cells. 20 nm SiO_2 nanoparticles were more toxic than 50 nm SiO_2 nanoparticles. The possible reason could be related to the depletion of glutathione (GSH, a tripeptide responsible for the homeostasis of free radicals in cells) and the increase of ROS, and smaller particles with higher surface area tend to trigger higher level of GSH decrease

in cells. Horie *et al.* (Horie et al. 2009) showed similar results that smaller TiO_2 nanoparticles tend to adsorb more proteins and cause severe toxic effect to human keratinocyte HaCaT cells and human lung carcinoma A549 cells. However their explanation was that the cytotoxicity of TiO_2 nanoparticles was due to the depletion of proteins in the cell culture medium. But based on our data, even 300 μg/ml of TiO_2 nanoparticles did not cause obvious decrease of proteins in the cell culture medium (data not shown here). So the size dependent cytotoxicity of TiO_2 nanoparticles is less likely due to nutrient depletion. Instead, the adsorption, denaturalization or even the damage of biomolecules could be a more reasonable explanation.

Thus, our studies demonstrated that the particles size can influence the cytotoxicity of nanoparticles. Smaller particles tend to have higher cytotoxicity, as smaller particles have more molecules exposed on the surface of particles to interact with surrounding biomolecules such as proteins. The protein adsorption could be an important paradigm to predict the *in vitro* cytotoxicity of nanoparticles, especially for low toxic nanoparticles such as PLGA and TiO_2 nanoparticles. The identification of the intracellular biomolecules attached on PLGA and TiO_2 nanoparticles is a proposed study in the future. Understanding the interaction between biomolecules and specific nanoparticles will guide *in vitro* and *in vivo* studies to understand mechanism behind the toxicity of nanoparticles. These studies will have great potential to be utilized in the prediction of cytotoxicity of different nanoparticles in an abiotic condition.

4. Conclusions

In this study, we observed size dependent cytotoxicity of both PLGA and TiO_2 nanoparticles. Biomedical used PLGA nanoparticles did not exhibit strong cytotoxic effect when compared with TiO_2 nanoparticles but the potential of smaller PLGA nanoparticles to trigger the release of TNF-α should not be ignored, especially for clinical applications. 200 nm PLGA nanoparticles did not trigger any negative response from cells based on our current results, but more studies are still needed to evaluate the biocompatibility of PLGA nanoparticles before they can be used in human body. Higher cytotoxic effect was observed in cells treated with TiO_2 nanoparticles, especially at concentration higher than 100μg/ml. The damages include generation of ROS, mitochondrial depolarization, plasma membrane leakage, increased intracellular calcium concentration and inflammation response. The size-dependent cytotoxicity of both PLGA and

TiO_2 nanoparticles could be due to the fact that smaller particles with larger specific surface area could adsorb more biomolecules such as proteins in the environment. Thus the ability to adsorb proteins could be an important paradigm to predict the *in vitro* cytotoxicity of nanoparticles, especially for low toxic nanoparticles such as PLGA and TiO_2 nanoparticles.

Acknowledgements

Ms Xiong Sijing would like to acknowledge the Nanyang Technological University - Ian Ferguson Postgraduate Fellowship support for her research attachment to University of California, Los Angeles (UCLA). We thank Dr. Andre E. Nel and Dr. Tian Xian (UC Center for Environmental Implications of Nanotechnology) for their kind help in this study. Financial support from the following funding agencies (NMRC, A*STAR and NITHM) are also acknowledged: NMRC/EDG/0062/2009 and A*STAR Project No: 102 129 0098.

Conflict of interest

The authors declare that they have no conflict of interest.

References

Brookes PS, Yoon YS, Robotham JL, Anders MW, Sheu SS (2004) Calcium, ATP, and ROS: a mitochondrial love-hate triangle. Am J Physiol-Cell Physiol 287 (4):C817-C833. doi:10.1152/ajpcell.00139.2004

Cartiera MS, Johnson KM, Rajendran V, Caplan MJ, Saltzman WM (2009) The uptake and intracellular fate of PLGA nanoparticles in epithelial cells. Biomaterials 30(14):2790–2798

Chorny M, Fishbein I, Danenberg HD, Golomb G (2002) Lipophilic drug loaded nanospheres prepared by nanoprecipitation: effect of formulation variables on size, drug recovery and release kinetics. Journal of Controlled Release 83 (3):389-400

de Lima R, do Espirito Santo Pereira A, Porto R, Fraceto L (2010) Evaluation of cyto- and genotoxicity of poly(lactide-co-glycolide) nanoparticles. Journal of Polymers and the Environment:1-7. doi:10.1007/s10924-010-0262-4

Deng ZJ, Liang MT, Monteiro M, Toth I, Minchin RF (2011) Nanoparticle-induced unfolding of fibrinogen promotes Mac-1 receptor activation and inflammation. Nat Nanotechnol 6 (1):39-44. doi:10.1038/nnano.2010.250

Ding T (2009) Study on MCP-1 related to inflammation induced by biomaterials. Biomedical materials 4 (3)

Dong Y, Feng SS (2007) Poly(D, L-lactide-co-glycolide) (PLGA) nanoparticles prepared by high pressure homogenization for paclitaxel chemotherapy. Int J Pharm 342(1–2):208–214. doi: 10.1016/j.ijpharm.2007.04.031

Duvvuri S, Janoria KG, Mitra AK (2005) Development of a novel formulation containing poly(d,l-lactide-co-glycolide) microspheres dispersed in PLGA-PEG-PLGA gel for sustained delivery of ganciclovir. Journal of Controlled Release 108:282-293

George S, Pokhrel S, Xia T, Gilbert B, Ji Z, Schowalter M, Rosenauer A, Damoiseaux R, Bradley KA, Mädler L, Nel AE (2009) Use of a rapid cytotoxicity screening approach to engineer a safer zinc oxide nanoparticle through iron doping. ACS Nano 4 (1):15-29. doi:10.1021/nn901503q

George S, Xia T, Rallo R, Zhao Y, Ji Z, Lin S, Wang X, Zhang H, France B, Schoenfeld D, Damoiseaux R, Liu R, Lin S, Bradley KA, Cohen Y, Nel AE (2011) Use of a high-throughput screening approach coupled with in vivo zebrafish embryo screening to develop hazard ranking for engineered nanomaterials. ACS Nano 5 (3):1805-1817. doi:10.1021/nn102734s

Gurr J-R, Wang ASS, Chen C-H, Jan K-Y (2005) Ultrafine titanium dioxide particles in the absence of photoactivation can induce oxidative damage to human bronchial epithelial cells. Toxicology 213 (1-2):66-73

Heng BC, Zhao X, Xiong S, Ng KW, Boey FY-C, Loo JS-C (2010a) Toxicity of zinc oxide (ZnO) nanoparticles on human bronchial epithelial cells (BEAS-2B) is accentuated by oxidative stress. Food and Chemical Toxicology 48 (6):1762-1766

Heng BC, Zhao X, Xiong S, Ng KW, Boey FYC, Loo JSC (2010b) Cytotoxicity of zinc oxide (ZnO) nanoparticles is influenced by cell density and culture format. Archives of Toxicology 85 (6):695-704. doi:10.1007/s00204-010-0608-7

Horie M, Nishio K, Fujita K, Endoh S, Miyauchi A, Saito Y, Iwahashi H, Yamamoto K, Murayama H, Nakano H, Nanashima N, Niki E, Yoshida Y (2009) Protein adsorption of

ultrafine metal oxide and its influence on cytotoxicity toward cultured cells. Chemical Research in Toxicology 22 (3):543-553. doi:10.1021/tx800289z

Jang HD, Kim S-K, Kim S-J (2001) Effect of particle size and phase composition of titanium dioxide nanoparticles on the photocatalytic properties. Journal of Nanoparticle Research 3 (2):141-147. doi:10.1023/a:1017948330363

Kang JL, Moon C, Lee HS, Lee HW, Park EM, Kim HS, Castranova V (2008) Comparison of the biological activity between ultrafine and fine titanium dioxide particles in RAW 264.7 cells associated with oxidative stress. J Toxicol Env Health Part A 71 (8):478-485. doi:10.1080/15287390801906675

Long TC, Saleh N, Tilton RD, Lowry GV, Veronesi B (2006) Titanium dioxide (P25) produces reactive oxygen species in immortalized brain microglia (BV2): Implications for nanoparticle neurotoxicity. Environmental Science and Technology 40 (14):4346-4352

McCall MJ (2011) Environmental, health and safety issues Nanoparticles in the real world. Nat Nanotechnol 6 (10):613-614

Nel A, Xia T, Madler L, Li N (2006) Toxic potential of materials at the nanolevel. Science 311 (5761):622-627. doi:10.1126/science.1114397

Ng KW, Khoo SPK, Heng BC, Setyawati MI, Tan EC, Zhao X, Xiong S, Fang W, Leong DT, Loo JSC (2011) The role of the tumor suppressor p53 pathway in the cellular DNA damage response to zinc oxide nanoparticles. Biomaterials 32 (32):8218-8225

Oberdörster G, Maynard A, Donaldson K, Castranova V, Fitzpatrick J, Ausman K, Carter J, Karn B, Kreyling W, Lai D, Olin S, Monteiro-Riviere N, Warheit D, Yang H, Group ArftIRFRSINTSW (2005a) Principles for characterizing the potential human health effects from exposure to nanomaterials: elements of a screening strategy. Particle and Fibre Toxicology 2 (1):8

Oberdörster G, Oberdörster E, Oberdörster J (2005b) Nanotoxicology: An emerging discipline evolving from studies of ultrafine particles. Environ Health Perspect 113 (7):823-839. doi:10.1289/ehp.7339

Oberdorster G, Ferin J, Gelein R, Soderholm SC, Finkelstein J (1992) Role of the alveolar macrophage in lung injury - studies with ultrafine particles Environmental Health Perspectives 97:193-199. doi:10.2307/3431353

Palomaki J, Karisola P, Pylkkanen L, Savolainen K, Alenius H (2009) Engineered nanornaterials cause cytotoxicity and activation on mouse antigen presenting cells. Toxicology 267 (1-3):125-131. doi:10.1016/j.tox.2009.10.034

Park E-J, Yi J, Chung K-H, Ryu D-Y, Choi J, Park K (2008) Oxidative stress and apoptosis induced by titanium dioxide nanoparticles in cultured BEAS-2B cells. Toxicology Letters 180 (3):222-229

Petkovic J, Zegura B, Stevanovic M, Drnovsek N, Uskokovic D, Novak S, Filipic M (2010) DNA damage and alterations in expression of DNA damage responsive genes induced by TiO(2) nanoparticles in human hepatoma HepG2 cells. Nanotoxicology 5 (3):341-353. doi:10.3109/17435390.2010.507316

Rahman Q, Lohani M, Dopp E, Pemsel H, Jonas L, Weiss DG, Schiffmann D (2002) Evidence that ultrafine titanium dioxide induces micronuclei and apoptosis in syrian hamster embryo fibroblasts. Environmental Health Perspectives 110 (8):797-800

Sayes CM, Wahi R, Kurian PA, Liu Y, West JL, Ausman KD, Warheit DB, Colvin VL (2006) Correlating nanoscale titania structure with toxicity: A cytotoxicity and inflammatory

response study with human dermal fibroblasts and human lung epithelial cells. Toxicological Sciences 92 (1):174-185

Semete B, Booysen L, Lemmer Y, Kalombo L, Katata L, Verschoor J, Swai HS (2010) In vivo evaluation of the biodistribution and safety of PLGA nanoparticles as drug delivery systems. Nanomedicine: Nanotechnology, Biology and Medicine 6 (5):662-671

Shang W, Nuffer JH, Dordick JS, Siegel RW (2007) Unfolding of Ribonuclease A on Silica Nanoparticle Surfaces. Nano Letters 7 (7):1991-1995. doi:10.1021/nl070777r

Sim RB, Wallis R (2011) Surface properties: Immune attack on nanoparticles. Nat Nano 6 (2):80-81

Skocaj M, Filipic M, Petkovic J, Novak S (2011) Titanium dioxide in our everyday life; is it safe? Radiol Oncol 45 (4):227-247. doi:10.2478/v10019-011-0037-0

Song X, Zhao Y, Wu W, Bi Y, Cai Z, Chen Q, Li Y, Hou S (2008) PLGA nanoparticles simultaneously loaded with vincristine sulfate and verapamil hydrochloride: Systematic study of particle size and drug entrapment efficiency. Int J Pharm 350 (1-2):320-329

Tanaka Y, Suganuma M (2001) Effects of heat treatment on photocatalytic property of sol-gel derived polycrystalline TiO2. J Sol-Gel Sci Technol 22 (1-2):83-89. doi:10.1023/a:1011268421046

Tao F, Kobzik L (2002) Lung macrophage-epithelial cell interactions amplify particle-mediated cytokine release. Am J Respir Cell Mol Biol 26 (4):499-505

Teichroeb J, Forrest J, Jones L (2008) Size-dependent denaturing kinetics of bovine serum albumin adsorbed onto gold nanospheres. The European Physical Journal E: Soft Matter and Biological Physics 26 (4):411-415. doi:10.1140/epje/i2007-10342-9

Wang F, Gao F, Lan M, Yuan H, Huang Y, Liu J (2009) Oxidative stress contributes to silica nanoparticle-induced cytotoxicity in human embryonic kidney cells. Toxicology in Vitro 23 (5):808-815

Wang JJ, Sanderson BJS, Wang H (2007) Cyto- and genotoxicity of ultrafine TiO2 particles in cultured human lymphoblastoid cells. Mutation Research/Genetic Toxicology and Environmental Mutagenesis 628 (2):99-106

Wang WR, Zhu RR, Xiao R, Liu H, Wang SL (2010) The electrostatic interactions between nano-TiO(2) and trypsin inhibit the enzyme activity and change the secondary structure of trypsin. Biol Trace Elem Res 142 (3):435-446. doi:10.1007/s12011-010-8823-x

Xia T, Kovochich M, Brant J, Hotze M, Sempf J, Oberley T, Sioutas C, Yeh JI, Wiesner MR, Nel AE (2006) Comparison of the abilities of ambient and manufactured nanoparticles to induce cellular toxicity according to an oxidative stress paradigm. Nano Letters 6 (8):1794-1807

Xia T, Kovochich M, Liong M, Mädler L, Gilbert B, Shi H, Yeh JI, Zink JI, Nel AE (2008) Comparison of the mechanism of toxicity of zinc oxide and cerium oxide nanoparticles based on dissolution and oxidative stress properties. ACS Nano 2 (10):2121-2134. doi:10.1021/nn800511k

Zhang H, Xia T, Meng H, Xue M, George S, Ji Z, Wang X, Liu R, Wang M, France B, Rallo R, Damoiseaux R, Cohen Y, Bradley KA, Zink JI, Nel AE (2011) Differential expression of syndecan-1 mediates cationic nanoparticle toxicity in undifferentiated versus differentiated normal human bronchial epithelial cells. ACS Nano 5 (4):2756-2769. doi:10.1021/nn200328m

Zhang N, Chittasupho C, Duangrat C, Siahaan TJ, Berkland C (2007) PLGA nanoparticle-peptide conjugate effectively targets intercellular cell-adhesion molecule-1. Bioconjugate Chemistry 19 (1):145-152. doi:10.1021/bc700227z

Zhao X, Ng S, Heng BC, Guo J, Ma L, Tan TTY, Ng KW, Loo SCJ (2012) Cytotoxicity of hydroxyapatite nanoparticles is shape and cell dependent. Archives of Toxicology:1-16. doi:10.1007/s00204-012-0827-1

Zhao XX, Heng BC, Xiong SJ, Guo J, Tan TTY, Boey FYC, Ng KW, Loo JSC (2010) In vitro assessment of cellular responses to rod-shaped hydroxyapatite nanoparticles of varying lengths and surface areas. Nanotoxicology 5 (2):182-194. doi:10.3109/17435390.2010.503943

Ziolli RL, Jardim WF (2002) Photocatalytic decomposition of seawater-soluble crude-oil fractions using high surface area colloid nanoparticles of TiO2. Journal of Photochemistry and Photobiology A: Chemistry 147 (3):205-212

Table 1 Fluorescent probes used in this study

Marker	**Probe**	**Ex/Em wavelength (nm)**	**Utility**
Cell nucleus	Hoechst	355/465	Localization of cells
Plasma membrane damage	PI	540/620	Damaged integrity of plasma membrane
Mitochondrial superoxide	MitoSOX	510/580	Generation of mitochondrial superoxide
Mitochondrial membrane potential	JC-1	480/530-590	Mitochondrial depolarization
Intracellular calcium	Fluo-4	480/510	Increase of intracellular Ca^{2+} concentration

Table 2 Characterization results of PLGA and TiO_2 nanoparticles with different particle size

		P60	P100	P200	T10	T20	T100
Primary Particle Size (nm)		61	94	205	10	20	100
water	Size (nm)	101	149	207	669	307	349
	PDI	0.046	0.097	0.071	0.186	0.263	0.224
	Zeta Potential (mV)	-17.0	-21.4	-22.9	-16.9	32.3	19.1
CDMEM	Size (nm)	192	120	196	262	338	444
	PDI	0.379	0.246	0.212	0.005	0.180	0.248
	Zeta Potential (mV)	-2.7	-6.7	-5.0	-5.7	-7.7	-9.3
BEGM	Size (nm)	536	158	233	1457	707	1336
	PDI	0.343	0.131	0.110	0.298	0.289	0.255
	Zeta Potential (mV)	-6.4	-9.6	-3.6	-11.0	-12.1	-9.9
Theoretical Surface Area (m^2/g)		72	46	22	154	73	15
BET Surface Area (m^2/g)		/	/	/	166.0	50.4	17.2
Cristal structure		/	/	/	Anatase	A*/R* 81/19	Anatase
Endotoxin (EU/ml)		<0.06	<0.06	<0.06	<0.06	<0.06	<0.06

A^* represents anatase
R^* represents rutile

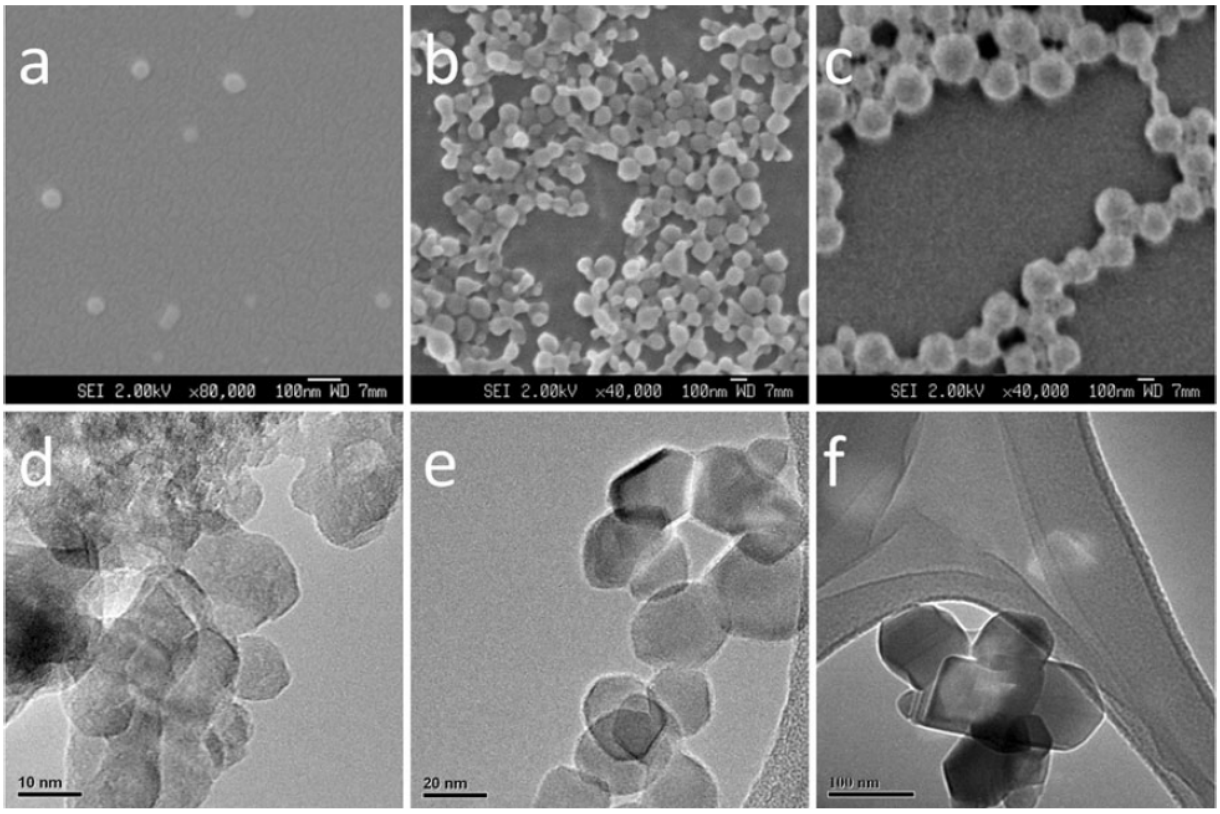

Fig. 1 SEM micrographs of 3 spherical PLGA nanoparticle samples with different sizes (a) P60, PLGA nanoparticles of size 61 nm , scale bar 100 nm; (b) P100, PLGA nanoparticles of size 94 nm, scale bar 100 nm; (c) P200, PLGA nanoparticles of size 205 nm, scale bar 100 nm. TEM images of TiO_2 nanoparticles of 3 different sizes (d) T10, TiO_2 nanoparticles of size 10 nm, scale bar 10 nm; (e) T20, TiO_2 nanoparticles of size 20 nm, scale bar 20 nm; (f) T100, TiO_2 nanoparticles of size 100 nm, scale bar 100 nm.

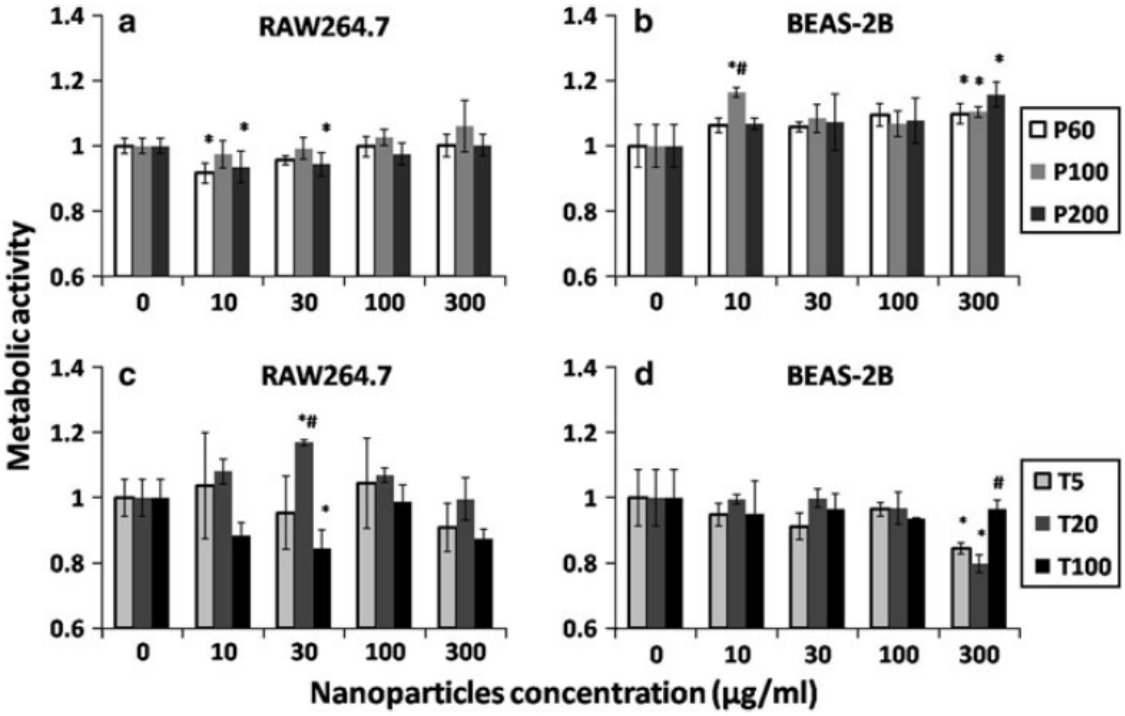

Fig. 2 The metabolic activity of live cells after cells were incubated with PLGA and TiO_2 nanoparticles for 24 h. The metabolic activity of cells was quantified by MTS assay and normalized to negative control (0 μg/ml). (a) RAW264.7 cells after incubation with PLGA nanoparticles of three different sizes (b) BEAS-2B cells after incubation with PLGA nanoparticles of three different sizes (c) RAW264.7 cells after incubation with TiO_2 nanoparticles of three different sizes (d) BEAS-2B cells after incubation with TiO_2 nanoparticles of three different sizes. The data represents means ± SD, n=4. * p<0.05 compared control (0 μg/ml). # p<0.05 compared with other two particles in the same concentration.

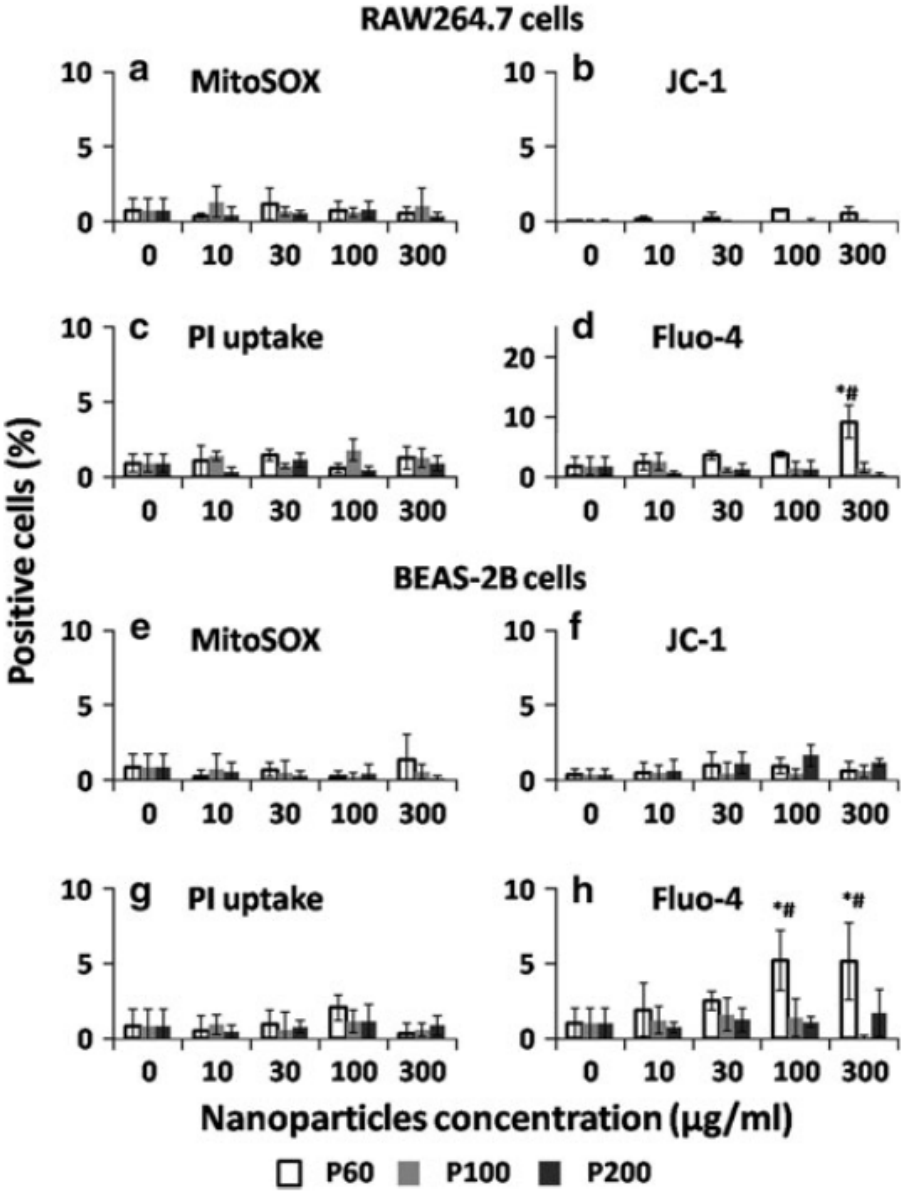

Fig. 3 Multiparametric assays to detect the *in vitro* cytotoxicity of different sized PLGA nanoparticles after 24 h incubation with (a to d) RAW264.7 and (e to h) BEAS-2B cells. The concentration ranges from 10 µg/ml to 300 µg/ml. The cells were stained for 30 min with the dye cocktails to assay for (a & e) MitoSOX staining, (b & f) JC-1 staining, (c & g) PI uptake and (d & h) Fluo-4 staining. The percentage of cells showed positive fluorescence above a certain threshold was recorded by using MetaXpress software. The data represents means ± SD, n=4. * $p<0.05$ compared control (0 µg/ml). # $p<0.05$ compared with other two particles in the same concentration.

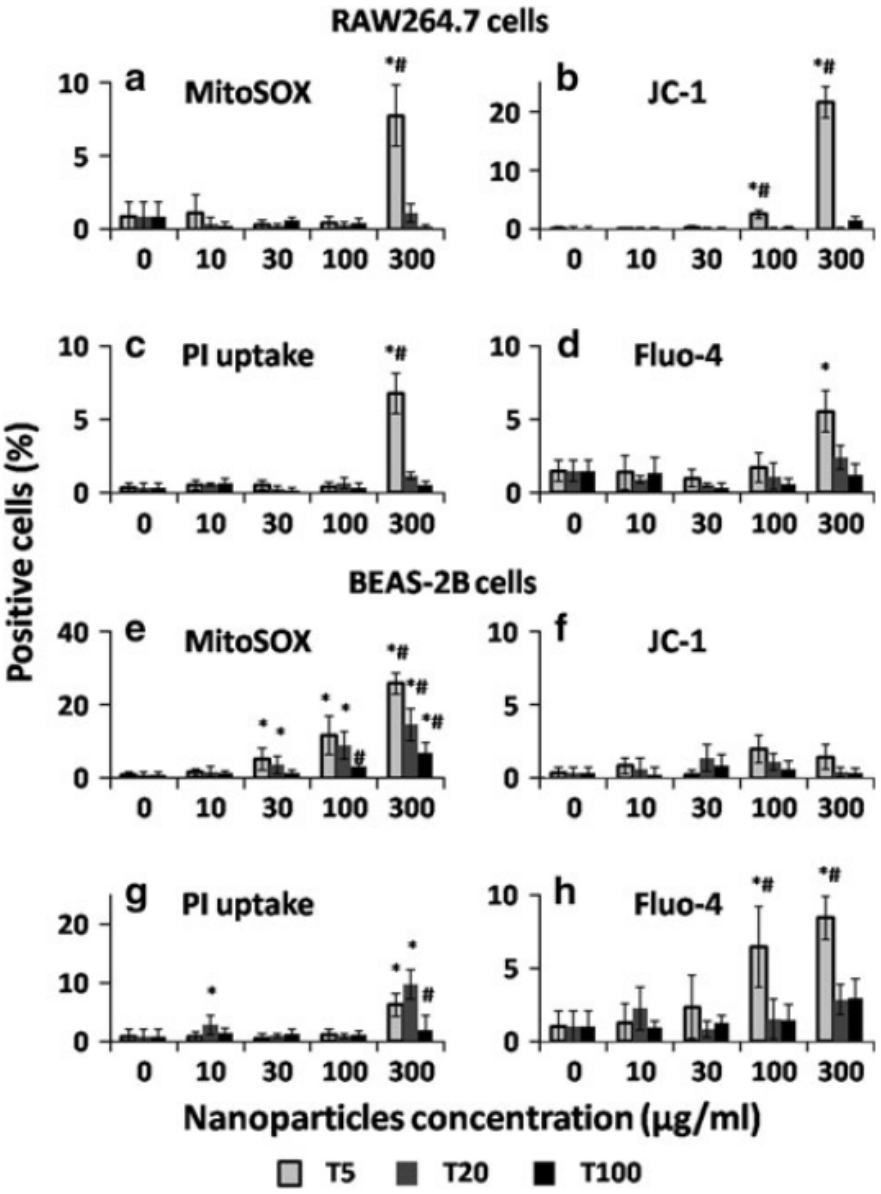

Fig. 4 Multiparametric assays to detect the *in vitro* cytotoxicity of different sized TiO_2 nanoparticles after 24 h incubation with (a to d) RAW264.7 and (e to h) BEAS-2B cells. The concentration ranges from 10 µg/ml to 300 µg/ml. The cells were stained for 30 min with the dye cocktails to assay for (a & e) MitoSOX staining, (b & f) JC-1 staining, (c & g) PI uptake and (d & h) Fluo-4 staining. The percentage of cells showed positive fluorescence above a certain threshold was recorded by using MetaXpress software. The data represents means ± SD, n=4. * $p<0.05$ compared control (0 µg/ml). # $p<0.05$ compared with other two particles in the same concentration.

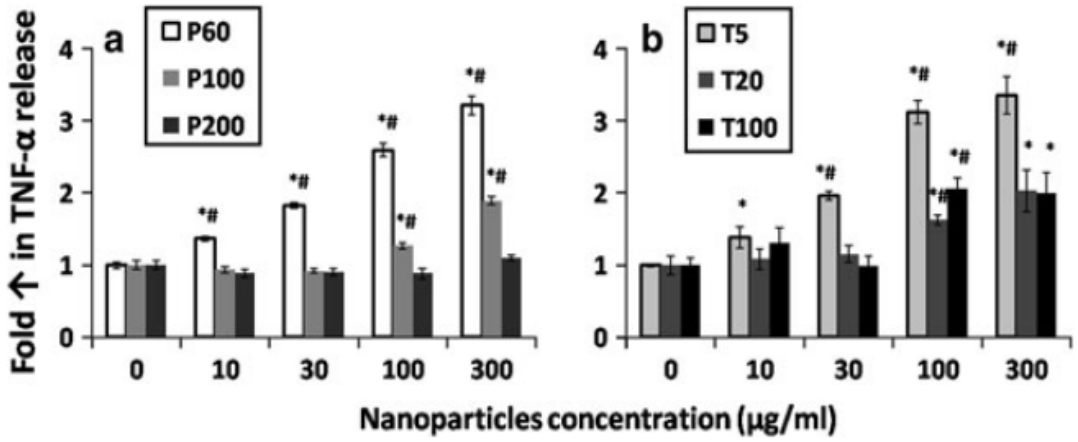

Fig. 5 The TNF-α released from RAW264.7 cells after the cells were stimulated by (A) PLGA and (B) TiO_2 nanoparticles for 24 h. The TNF-α released from macrophages into medium was measured by ELISA and normalized to negative control (0 μg/ml). The data represents means ± SD, n=4. * p<0.05 compared control (0 μg/ml). # p<0.05 compared with other two particles in the same concentration.

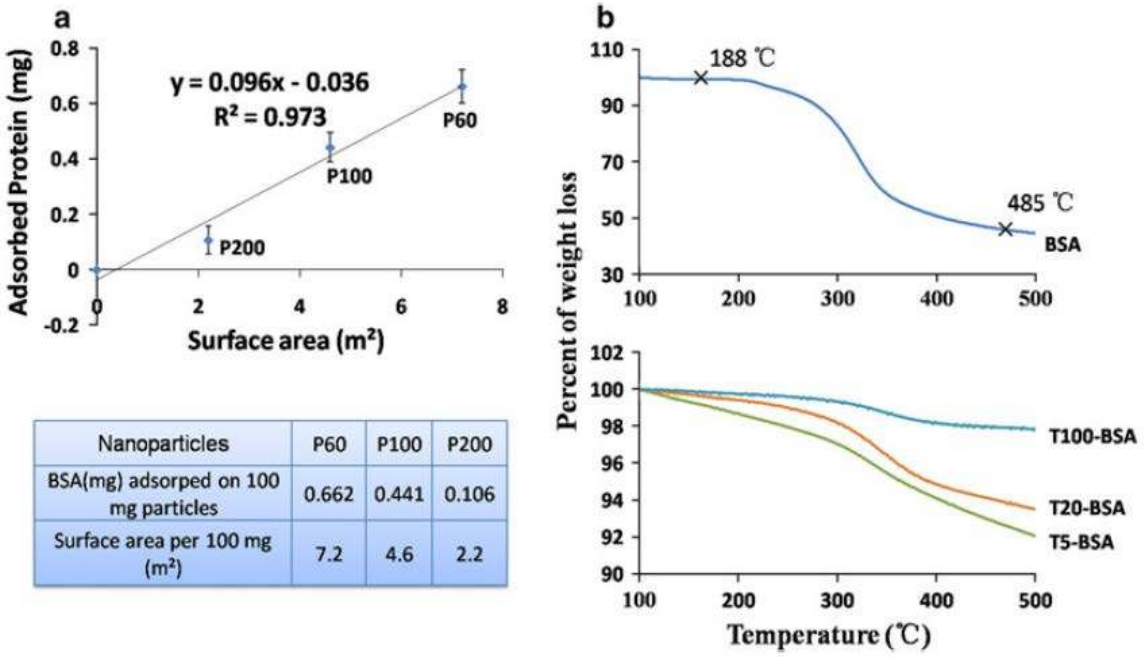

Nanoparticles	P60	P100	P200
BSA(mg) adsorped on 100 mg particles	0.662	0.441	0.106
Surface area per 100 mg (m^2)	7.2	4.6	2.2

Fig. 6 (A) Protein quantification of BSA attached on PLGA nanoparticles through Pierce 660 assay. The data represents mean ± SD, n=4. (B) TGA analysis of BSA adsorption on TiO_2 nanoparticles. T10-BSA, T20-BSA and T100-BSA represent the weight decrease of particles after interaction with protein BSA. This indicated more BSA adsorbed onto T10 and T20 nanoparticles than on relatively larger T100 nanoparticles.

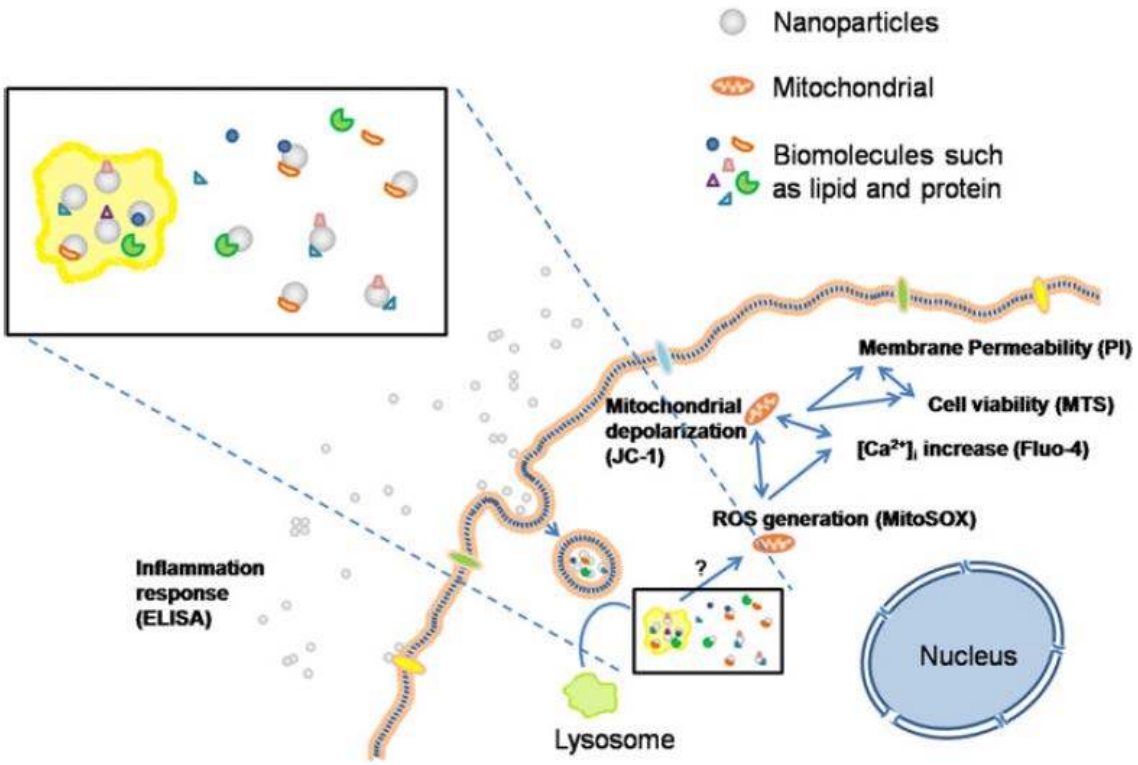

Fig. 7 Schematic of the possible mechanism behind the size dependent cytotoxicity of PLGA and TiO_2 nanoparticles